Journal of Ceramic Processing Research. Vol. 14, No. 5, pp. 641~647 (2013)

J O U R N A L O F
Ceramic Processing Research

Consolidation and mechanical properties of ultra fine WC-5 wt.% carbides hard materials by a rapid sintering method

In-Jin Shon[a], Ik-Hyun Oh[b], Jung-Han Ryu[b], Jun-Ho Jang[b], Hee-Jun Youn[b] and Hyun-Kuk Park[a,b,*]

[a]*Division of Advanced Materials Engineering and the Research Center of Advanced Materials Development, Engineering College, Chonbuk National University 541-756, Korea*

[b]*Korea Institute of Industrial Technology (KITECH), 1110-9 Oryong-dong, Buk-gu, Gwang-ju, Korea*

Using the pulsed current activated sintering method, WC-5 wt.% carbides hard materials were densified using an ultra-fine WC-NbC, TaC, TiC and ZrC powder. The WC-carbides were nearly completely dense with a relative density of up to 99% after the simultaneous application of 60 MPa of pressure and about 10 minutes of electric current without significant change in the grain size. The average grain size of WC that was produced through PCAS was approximately 500 nm. The hardness and fracture toughness of the dense WC-Carbide composites were also investigated.

Key words: Rapid Sintering, WC-binders, Hard Material, Mechanical Properties, Pulsed Current Activated Sintering.

Introduction

Many of the transition metal carbides (e.g., WC, NbC, TaC, TiC and ZrC) are high melting-temperature compounds with high hardness, high thermal and electrical conductivities, and a relatively high chemical stability. They are primarily used as cutting tools and abrasive materials in single-phase and composites. In the latter case, their use as cemented carbides involves the formation of a composite with a binder metal, such as Co or Ni. Tungsten carbide has a high melting point and high hardness [1, 2]. In addition to its use as a cutting material, it has been considered for other uses such as a catalyst (substituting for noble metals) [3-5], as a catalyst electrode in fuel cells, and as a coating for aerospace components [6].

Cemented carbides are widely used for wear parts in various applications, i.e., face seals, tools for metal cutting and rock drilling. Binderless carbides have been developed as a complement to conventional cemented carbides for use in corrosive environments where the metal binder degrades [7]. Normally binderless carbides have a lower abrasion resistance than metal-rich cemented carbides, however higher than that of common engineering ceramics. The main advantages of the materials over other ceramics in wear applications is its ability to withstand high pressures and speed in sliding contact without microfracturin [8].

When conventional sintering processes are used to sinter nano-sized powders, concomitant grain growth leads to the destruction of the nanostructure. This focuses attention on consolidation methods in which grain growth can be eliminated or significantly reduced. To accomplish this, rapid sintering methods have been widely used to sinter nano-sized powders. The most obvious advantage of rapid sintering is that fast heating and cooling rates, and short dwell times lead to bypassing low-temperature, non-densifying mass transport (e.g., surface diffusion) [9, 10]. However, conventional rapid heating can lead to temperature gradients and thus differential densification (non-uniform microstructures), low density, or specimen cracking. To overcome these difficulties, other rapid sintering techniques, such as the high-frequency induction heated sintering (HFIHS) [11-13], have been developed.

So, controlling the grain growth during sintering is a key component to the commercial success of nanostructured WC-carbide composites. In this study, WC-carbides were sintered using a rapid sintering process that is known as pulsed current activated sintering. This method combines a pulsed current with the application of a high pressure. The goal of this study was to produce dense, ultra-fine WC-5 wt.% carbide hard materials in very short sintering times (< 10 minutes). Additionally, the mechanical properties of the WC hard materials were investigated.

Experimental Procedure

In this study, 99.95% pure tungsten carbide (0.4 ~ 0.5 μm, TaeguTec Ltd.), 99.5% pure Niobium carbide (< 10 μm, Alfa Products), 99.5% pure Tantalnum carbide (–325 mesh, Alfa Products), 99.5% pure Titanium carbide (2 μm, Alfa Products), 99.5%

*Corresponding author:
Tel : +82 62 600 6181
Fax: +82 62 600 6149
E-mail: hk-park@kitech.re.kr

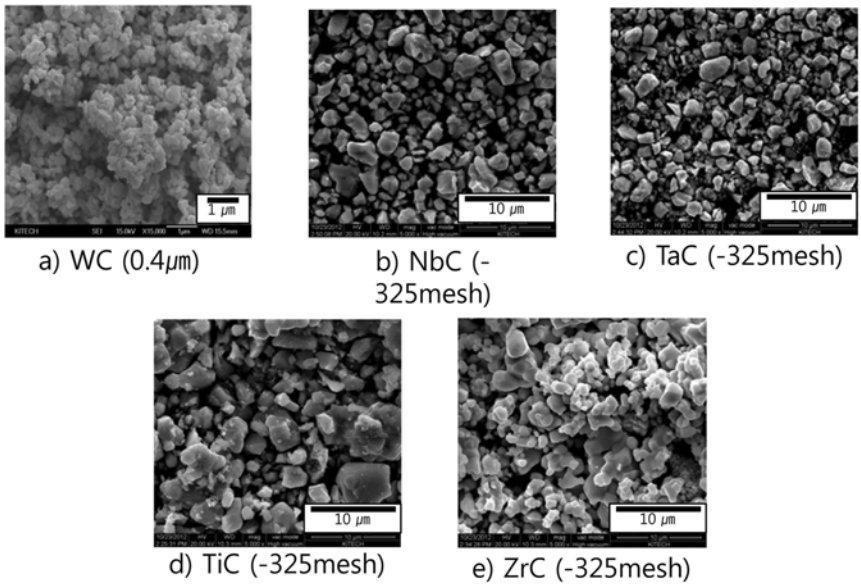

Fig. 1. FE-SEM images of the raw materials; (a) WC, (b) NbC, (c) TaC, (d) TiC and (e) ZrC.

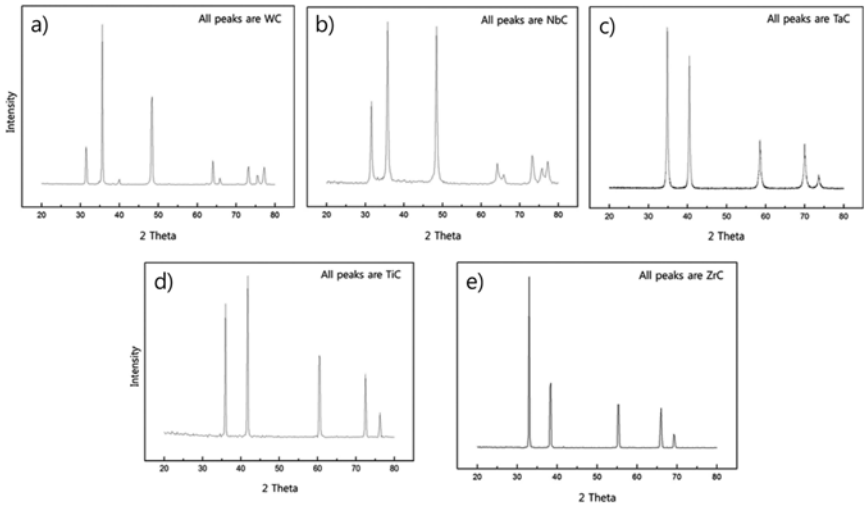

Fig. 2. XRD patterns of raw materials; (a) WC, (b) NbC, (c) TaC, (d) TiC and (e) ZrC.

pure zirconium carbide (–325 mesh, Alfa Products) powders were used as the starting materials. Figs. 1 and 2 show the FE-SEM images and XRD patterns of the raw materials that were used. The mixed WC and Carbide powder with a weight ratio of 95 : 5 was milled in a high energy ball mill (planetary mill) at 250 rpm for 10 hrs. Tungsten carbide balls (6 mm in diameter) were used in a sealed cylindrical stainless steel vial with alcohol. The weight ratio of the balls-to-powder was 10 : 1, and the alcohol-to powder-was 2 : 1. The milling significantly reduced the grain size of the powder. The grain size and the internal strain was calculated using Stokes and Wilson's formula [14]:

$$b = b_d + b_e = k\lambda / (d\cos\theta) + 4\varepsilon\tan\theta \quad (1)$$

where, b is the full width at half-maximum (FWHM) of the diffraction peak after the instrumental correction; b_d and b_e are the FWHM for a small grain size and

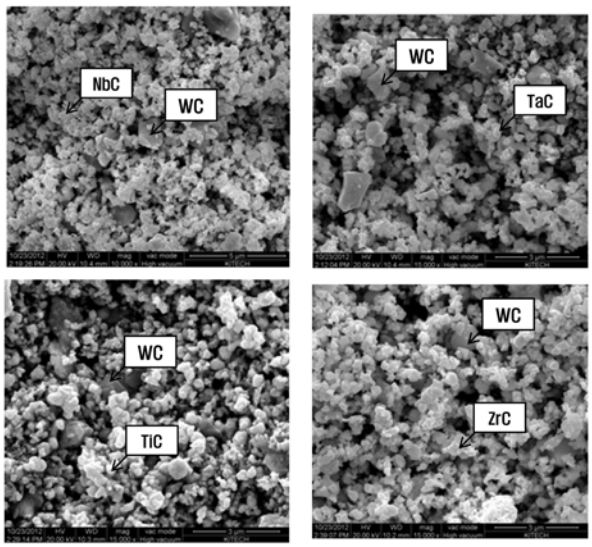

Fig. 3. FE-SEM images of milled WC-5 wt.% carbide powders; (a) NbC, (b) TaC, (c) TiC and (d) ZrC.

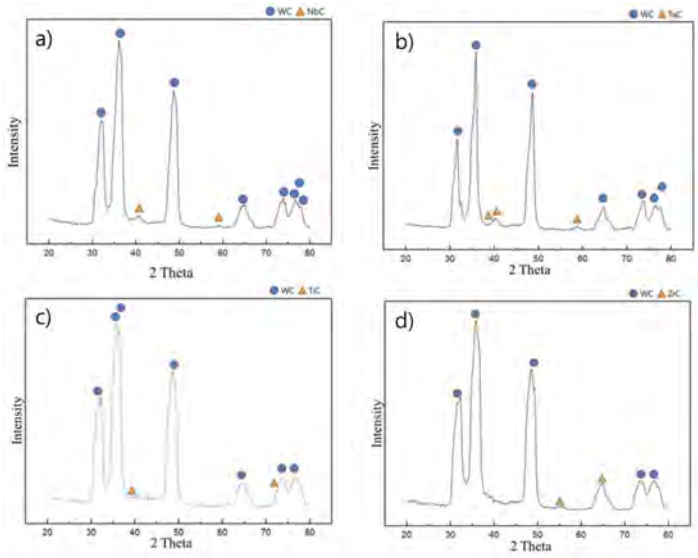

Fig. 4. XRD patterns of milled WC-5 wt.% carbide powders; (a) NbC, (b) TaC, (c) TiC and (d) ZrC.

internal strain, respectively; k is a constant (with a value of 0.9); λ is the wavelength of the X-ray radiation; d and ε are the grain size and the internal strain, respectively; and θ is the Bragg angle. The parameters b and bs follow Cauchy's form with the relationship: $B_0 = b + b_s$, where B_0 and b_s are the FWHM of the broadened Bragg peaks and a standard sample's Bragg peaks, respectively. Figs. 3 and 4 shows the FE-SEM and XRD patterns of the milled WC-5 wt.% Carbides powder mixture. The FWHM of the milled powder was greater than the raw powders due to the increase in the internal strain and the refinement of the grain size. The average grain sizes of the milled WC and NbC, TaC, TiC, ZrC powders were 284 and 210, 167, 195, 173 nm, respectively. After milling, the mixed powders were placed in a graphite die (outside diameter, 30 mm; inside diameter, 10 mm; height, 40 mm), and then placed into a rapid sintering system that was made by Sumitomo Coal Mining in Japan. A schematic diagram of this method is shown in Fig. 5. The PCAS apparatus included a 25 V, 1000 A DC power supply (which provided a pulsed current for 12 ms with an off time of 2 ms through the sample and die) and a 10 ton uniaxial press. First, the system was evacuated, and a uniaxial pressure of 60 MPa was applied. Then, a DC current was activated and maintained until the densification rate was negligible, as indicated by the observed shrinkage of the sample. The sample shrinkage was measured in real time using a linear gauge for the vertical displacement. The temperature was measured using a pyrometer that was focused on the surface of the graphite die. Depending on the heating rate, the electrical and thermal conductivities of the compact, and its relative density, the temperature on the surface and in the center of the sample could differ. The heating rate was approximately 100 Kminute^{-1} during this process. After the process was complete, the current was turned off, and the sample was allowed to cool to room temperature. The entire densification process using the PCAS technique consisted of four major control stages, including the chamber evacuation, pressure application, power application, and cool down. The four major sintering stages are schematically shown in Fig. 6. This process was carried out under a vacuum of 6 Pa. The relative densities of the sintered samples were measured using the Archimedes method. Microstructural information was obtained from the product samples, which were polished and etched using a Murakami's reagent (5 g $Fe_3(CN)_6$, 5 g NaOH, and 50 ml distilled water), for 60 to 150 sec at room temperature. The compositional and microstructural analyses of the products were carried out through X-ray diffraction (XRD) and field-emission scanning electron microscopy (FE-SEM).

The Vickers hardness was measured by performing indentation tests at a load of 30 kg and a dwell time

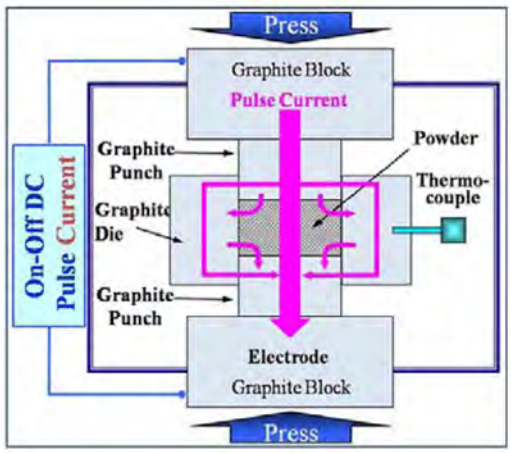

Fig. 5. Schematic diagram of apparatus for PCAS.

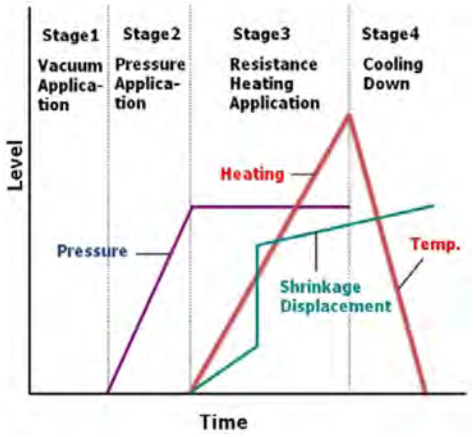

Fig. 6. Schematic representation of the temperature, pressure and shrinkage displacement profile during PCAS.

of 15 sec. The carbide grain size, d_{wc}, was obtained using the linear intercept method [15, 16].

Results and Discussion

The variations of shrinkage displacement and temperature with heating time during the sintering of WC-5 wt.% carbide hard materials using PCAS under a pressure of 60 MPa pressure are shown in Fig. 7. As the electric current is applied, the shrinkage displacement was nearly constant up to 600 °C, but then abruptly increased above this temperature. Fig. 8 shows the FE-SEM images of the WC-5 wt.% carbide samples that were heated to 1000 °C. The carbides were distributed homogeneously. Fig. 9 shows the XRD patterns of WC-5 wt.% carbide hard materials after sintering by PCAS in this work. For the WC-5 wt.% carbide hard materials, only carbide peaks were observed.

Two different methods were used to calculate the grain size (Stokes and Wilson's formula [14] and the linear intercept method). By the first expression, which was proposed by Stokes and Wilson's formula, the average grain sizes of WC were about 450, 483, 660, and 720 nm for the sintered WC-5 wt.% TaC, TiC, NbC and ZrC hard materials.

In the second expression, which was proposed by the linear intercept method, the sample surface preparation for the FE-SEM investigations was performed in accordance with the ASTM Method B657 for the metallographic determination of the microstructure in cemented carbides. Accordingly, the surface was polished in three steps. First, the samples were hand-ground on a 120 pm grade diamond grinder in order to remove at least 100 pm of the material. Then, a 6 pm grade grinder was used. Finally, the samples were polished using a 1 μm grade diamond paste**.** The surface was etched using Murakami's reagent for 60 to 150 sec at room temperature, then rinsed with alcohol and dried with acetone through ultra-sonication in order to identify the WC phase. Fig. 8 shows the FE-SEM images of the etched surfaces for the sample that was heated to 1000 °C at a pressure of 60 MPa. The structural parameters, i.e. the carbide grain size d_{wc} and the mean free path of the binder phase k (the average thickness of the binder phase), were obtained from the boundary intercepts with test lines on planar sections. The average number of intercepts per unit length of the test line was determined using the traces of the WC/carbide interface, $N_{WC/Carbide}$, and the carbide/carbide grain boundaries, $N_{WC/WC}$. From these quantities, the average carbide grain size and the mean free path were calculated using the following relationships [14, 15]:

$$d_{WC} = 2V_{WC}/(2N_{WC/WC} + N_{WC/carbide}) \quad (3)$$

where, V_{WC} is the carbide volume fraction, and $V_{Carbide}$

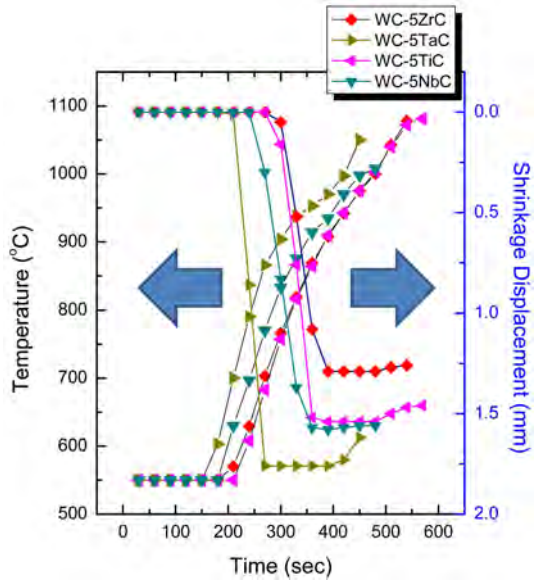

Fig. 7. Variations of temperature and shrinkage displacement with sintering time during PCAS of WC-5 wt.% carbide hard materials.

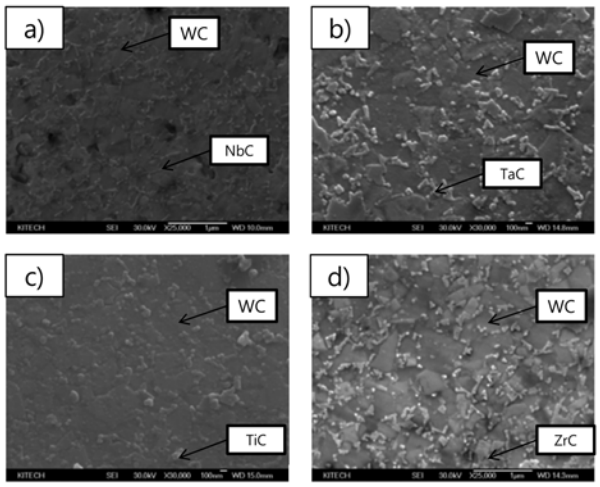

Fig. 8. FE-SEM images of etched surfaces of WC-5 wt.% carbides sintered by PCAS; (a) NbC, (b) TaC, (c) TiC and (d) ZrC.

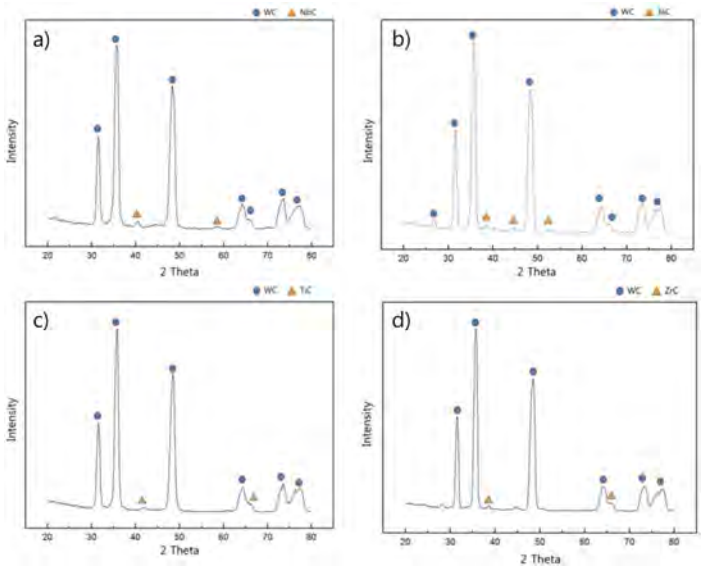

Fig. 9. XRD patterns of sintered WC-5 wt.% carbides: ; (a) NbC, (b) TaC, (c) TiC and (d) ZrC.

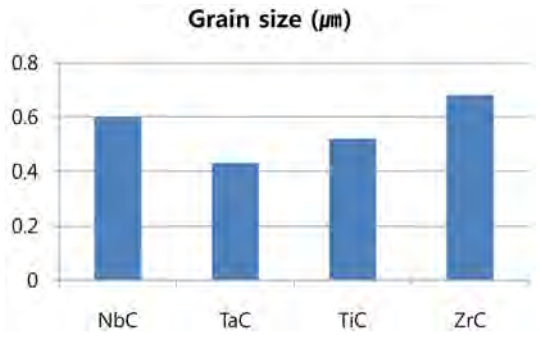

Fig. 10. Grain sizes of NbC, TiC, TaC and ZrC in WC-5 wt.% carbide hard materials produced by PCAS.

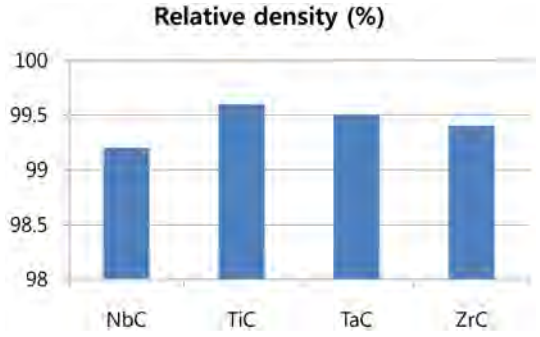

Fig. 11. Relative density of various WC-5 wt.% carbide hard materials produced by PCAS.

is the binder volume fraction. Fig. 10 shows the average grain size of various carbides (NbC, TiC, TaC and ZrC) in WC-5 wt.% carbide hard materials by PCAS. The grain sizes of TaC, TiC, NbC and ZrC were approximately 430, 460, 600, and 630 nm, respectively. However, the average grain size of WC in sintered WC-5 wt.% carbides was almost 500 nm and a fine structure was obtained without any grain growth during sintering using the PCAS method. Fig. 11 shows the relative density of WC-5 wt.% carbides. The WC-

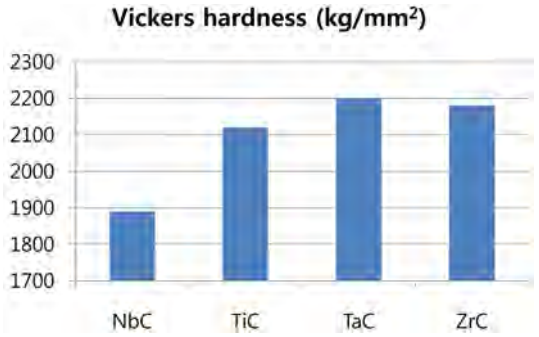

Fig. 12. Vickers hardness of various WC-5 wt.% carbide hard materials produced by PCAS.

5 wt.% carbides were almost completely dense with a relative density of up to 99%. Kim *et al*. [17] has reported that binderless WC was consolidated at 1500 ºC by high-frequency induction heated sintering and the sintering temperature of WC was decreased with the addition of TiC. In this study, the WC-5 wt.% carbides were consolidated at 1000 ºC lower than 1500 ºC. It was thought that various carbides (NbC, TiC, TaC and ZrC) were used as a carbide binder because they form the WC-carbide solid solution phase [18].

The Vickers hardness measurements were taken on the polished sections of WC-5 wt.% carbide hard materials using a 30 kgf load at a dwell time of 15 sec. At large enough loads, the indentations produced median cracks that emanated from the corners of the indent. The calculated Vickers hardness value of WC-5 wt.% carbide hard materials was shown in Fig. 12. The calculated Vickers hardness values of WC-5 wt.% TaC was the highest as 2200 kg/mm^2 among the WC-5 wt.% carbides.

The fracture toughness was calculated from the cracks that were produced from the indentations under

Table 1. Comparison of mechanical properties of WC-5 wt.% carbide sintered in this study with previously reported values.

Ref.	Binder contents (wt.%)	Relative density (%)	Grain Size (μm)	H_V (Kg/mm^2)	K_{IC} ($MPa \cdot m^{1/2}$)
[12]	9Co	99.4	0.26	1992	11.9
[13]	6Mo2C	99	0.45	2461	4.8
[18]	10Co	99.5	1.9	1333	13.5
[19]	10Ni	97.5	0.3	1810	13.5
This Study	5NbC	99.2	0.6	1890	7.43
	5TiC	99.6	0.46	2120	8.21
	5TaC	99.5	0.43	2200	7.68
	5ZrC	99.4	0.63	2180	8.12

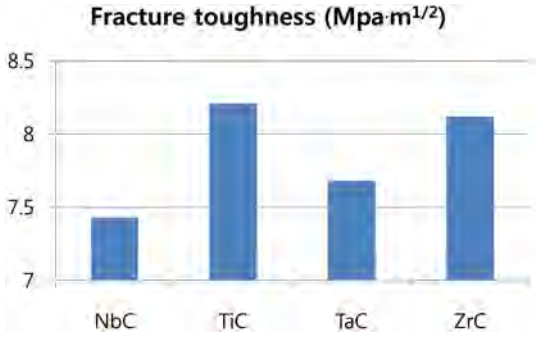

Fig. 13. Fracture toughness of various WC-5 wt.% carbide hard materials produced by PCAS.

large loads. The length of these cracks permits an estimation of the fracture toughness for the fracture toughness of the materials by mean of the expression [19]:

$$K_{IC} = 0.204(c/a)^{-3/2} H_v a^{1/2} \quad (4)$$

where, c is trace length of the crack measured from the center of the indentation, a is half of the average length of two indent diagonals, and H_v is the hardness. As with the hardness values, the toughness values were derived from the average of five measurements. The calculated fracture toughness values of WC-5 wt.% carbide hard materials were shown in Fig. 13. The calculated maximum fracture toughness values of WC-5 wt.% TiC was the highest as 8.2 $MPa \cdot m^{1/2}$ among the WC-5 wt.% carbides. Table 1 presents the calculated structural characteristics of the WC-binder composites, including the hardness and fracture toughness values, from the above formulas, based on the planar section measurements. In one of the reported studies [20], the WC-10Co sample was sintered at 1380 by the conventional method and in other reported studies [12, 13, 21], WC-9Co, $6Mo_2C$, and 10Ni samples were sintered at 1180, 1500 and 1340 by the high-frequency induction heated sintering method.

Summary

The WC-5 wt.% carbide hard materials were rapidly consolidated using the pulsed current activated sintering method with WC and NbC, TiC, TaC, ZrC powders. Almost fully dense WC-5wt.% carbides were obtained within 10 minutes. The densification temperature of WC was remarkably reduced through the addition of carbide. The grain sizes of NbC, TaC, TiC, and ZrC in WC-5 wt% carbides were approximately 600, 400, 500, and 630 nm, respectively, and the nano-structure was obtained without great grain growth during sintering using the PCAS method. The Vickers hardness values and fracture toughness values of WC-5 wt.% NbC, WC-5 wt.% TaC, WC-5 wt.% TiC and WC-5 wt.% ZrC were about 1890, 2200, 2120 and 2180 kg/mm^2 and 7.43, 7.68, 8.21 and 8.12 $MPa \cdot m^{1/2}$, respectively.

Acknowledgments

This research was supported by the Basic Science Research Program, through the National Research Foundation of Korea (NRF), funded by the Ministry of Education, Science and Technology (No. 2012001300), and this work was also supported by a grant of the Human Resources Development program (No. 2013 4030200330), of the Korea Institute of Energy Technology Evaluation and Planning (KETEP) grant funded by the Korea government Ministry of Trade, Industry and Energy.

References

1. P. Schwartzkopf, R. Kieffer, Refractory Hard Metals-Boride, Carbide, Nitride and Silicide, MacMillan, New York (1953).
2. L.E. Toth, Transition Metal Carbides and Nitrides, Academic Press, New York (1971).
3. L. Leclercq, M. Provost, H. Pastor, G. Grimblot, A.M. Hardy, L. Gengembre, J. Catalysis. 117 (1989) 371-383.
4. M.J. Ledoux, C.H. Pham, J. Guille, H. Dunlop, J. Catalysis. 134 (1992) 383-398.
5. L. Volpe, M. Boudart, J. Solid State Chem. 59 (1985) 348-356.
6. R. Koc, S.K. Kodambaka, J. Eur. Ceram. Soc. 20 (2000) 1859-1869.
7. S. Imasato, K. Tokumoto, T. Kitada, S. Kakaguchi, Int.

Refract. Met. Hard Mater. 13 (1995) 305-312.
8. H. Engqvist, N Axen, S. Hogmark, Tribol. Lett. 4 (1998) 251-258.
9. M.P. Harmer, R.J. Brook, J. Br. Ceram. Soc. 80 (1981) 147-149.
10. A. Morell, A. Mermosin, Bull. Am. Ceram. Soc. 59 (1980) 626-629.
11. Wonbaek Kim, Hee-Ji Wang, Ki-Min Roh, Sung-Wook Cho, Jae-Won Lim, and In-Jin Shon, Korean J. Met.Mater. 50 (2012) 310-315.
12. Song-Lee Du, In-Jin Shon, Jung-Mann Doh, Bang-Ju Park, and Jin-Kook Yoon, Korean J. Met. Mater. 50 (2012) 449-454.
13. In-Yong Ko, Na-Ra Park, and In-Jin Shon, Korean J. Met. Mater. Vol. 50, No. 5, (2012) 369-374.
14. F.L. Zhang, C.Y. Wang, M. Zhu, Scripta Mater. 49 (2003) 1123-1128.
15. Jia K, Fischer TE, Gallois G. Nanostruct Mater. 10 (1998) 875-891.
16. J.H. Han, D.Y. Kim, Acta Mater. 46 (1998) 2021-2028.
17. H.C. Kim, D.K. Kim, K.D. Woo, I.Y. Ko, I.J. Shon, International Journal of Refractory Metals & Hard Materials. 26 (2008) 48-54.
18. S. Imasato, K. Tokumoto, T. Kitada, S. Sakaguchi, International Journal of Refractory Metals & Hard Materials. 13 (1997) 305-312.
19. K. Niihara, J. Mater. Sci. Lett. 1 (1982) 12-16.
20. E.A. Almond, B. Roebuck,. Mat. Sci. Eng. A 105 (1988) 237-248.
21. H.C. Kim, I.J. Shon. J.K. Yoon, J.M. Doh, Z.A. Munir, Int. J. Ref. Met. & Hard Mat. 24 (2006) 427-431.